JOURNAL OF GUIDANCE, CONTROL, AND DYNAMICS
Vol. 34, No. 4, July–August 2011

Investigation of Practical Flight Envelope Protection Systems for Small Aircraft

W. Falkena,* C. Borst,* Q. P. Chu,† and J. A. Mulder‡
Delft University of Technology, 2629 HS Delft, The Netherlands

DOI: 10.2514/1.53000

Personal air transportation using small aircraft is a market that is expected to grow significantly in the near future. However, seventy times more accidents occur in this segment as compared with commercial aviation. The majority of these accidents is related to handling and control problems, which are closely linked to the experience level of the pilots. In commercial aviation, the combination of fly-by-wire technology and flight envelope protection is used to prevent these types of accidents. Instead of downscaling advanced and high-cost fly-by-wire platforms, a low-cost solution should be considered for the general aviation market. This paper focuses on a flight envelope protection system for small aircraft. Preliminary results are obtained from an empirical comparison study in the time domain between a proportional-integral-derivative-based control limiting approach, a command limiting approach, a constrained flight control law approach using model-based predictive control and incremental nonlinear dynamic inversion, and a virtual control limiting approach, which also uses incremental nonlinear dynamic inversion. Comparison is done not only using a nominal model but also in cases of parametric uncertainty, sensor noise, time delays, wind gusts, and turbulence. Investigation of the results reveals that, for this study, control limiting should be avoided, and for practical implementation command limiting is the best option.

Nomenclature

b	=	wing span
C_l	=	roll moment coefficient
C_m	=	pitch moment coefficient
C_n	=	yaw moment coefficient
C_X	=	aerodynamic force coefficient
C_Y	=	aerodynamic force coefficient
C_Z	=	aerodynamic force coefficient
$\mathbf{c}$	=	set of constraints
$\bar{c}$	=	mean aerodynamic chord
F	=	constraint matrix
$\mathbf{f}$	=	set of state functions
$\mathbf{g}$	=	set of input functions
H	=	transfer function
H_p	=	prediction horizon
H_u	=	input horizon
h	=	output function
J	=	inertia tensor, $\mathrm{kg} \cdot \mathrm{m}^2$
$\mathbf{K}$	=	set of aircraft states
K_d	=	differential gain
K_i	=	integral gain
K_p	=	proportional gain
k	=	discrete time
m	=	input dimension
$\mathbf{m_f}$	=	set of mapping functions
n	=	aircraft state dimension
p	=	roll rate, rad/s
Q	=	weighing matrix
q	=	pitch rate, rad/s
R	=	weighing matrix
r	=	yaw rate, rad/s
$\mathcal{S}$	=	convex region
T	=	time horizon, s
t	=	time, s
$\mathbf{U}$	=	set of possible inputs
$\mathcal{U}$	=	set of Lebesgue measurable functions
$\mathbf{u}$	=	input vector
V	=	velocity, m/s
$\mathbf{x}$	=	aircraft state vector
$\bar{x}$	=	upper limit of x
$\underline{x}$	=	lower limit of x
α	=	angle of attack, rad
β	=	angle of side-slip, rad
δ_a	=	aileron deflection, rad
δ_e	=	elevator deflection, rad
δ_r	=	rudder deflection, rad
ζ	=	linearized system state
θ	=	pitch angle, rad
ν	=	linearized system input
ϕ	=	roll angle, rad
ω	=	rotational velocity, rad/s

Presented as Paper 2010-7701 at the AIAA Guidance, Navigation, and Control Conference, Toronto, Ontario, Canada, 2–5 August 2010; received 1 November 2010; revision received 14 February 2011; accepted for publication 18 February 2011.

*Scientific Researcher, Control and Simulation Division, Faculty of Aerospace Engineering, Kluyverweg 1.

†Associate Professor, Control and Simulation Division, Faculty of Aerospace Engineering, Kluyverweg 1.

‡Scientific Director, Control and Simulation Division, Faculty of Aerospace Engineering, Kluyverweg 1.

I. Introduction

IN THE future airspace, a growth in small aircraft movements is to be expected, according to the United States small aircraft transportation system and the European personal air transportation system programs. The main reason for this growth is due to an increasing demand for people to reach more communities in less time. With the introduction of improved and cost-efficient technologies, it is even expected to become an attractive alternative to road transportation. In the general aviation segment, however, fatal and nonfatal accidents are not rare [1,2]. Currently, an average number of seven accidents per 100,000 flight hours dominates this segment. As this market is expected to grow significantly in future years, measures must be taken to guide this growth in a safe manner.

By looking more closely at accident analyses, frequent causes can be traced back to poor aircraft handling (72%) and pilot decision-making errors (36%) [1,2]. Simultaneously performing the tasks of aircraft handling, communication, navigation, and planning can be rather difficult, especially for less experienced pilots. In terms of

aircraft handling, misjudging the coupling of aircraft states and the effects of external disturbances can put pilots in unsafe regions of the flight envelope. In terms of decision making, ambiguous and conflicting information from the airborne systems can result in poor pilot "situation awareness" (SA) and decision making [3]. To resolve these issues, control-augmentation techniques can be used to create easy and safe aircraft handling characteristics, and new ways of using and presenting information on flight displays can be explored to improve SA and decision making [4,5]. This paper, however, only deals with improving flight safety by means of a flight envelope protection (FEP) control system that allows for a "carefree maneuvering" concept for small aircraft.

Commercial aviation has a long history of using control systems to shape ideal aircraft responses [6]. To increase safety, modern commercial aircraft, such as a Boeing 777 and an Airbus A380, are also equipped with FEP systems to protect against stall and exceeding overspeed and to limit load factors and angle of attack. These techniques have greatly reduced the handling and control accidents in the commercial aviation sector. However, simply downscaling these advanced fly-by-wire (FBW) platforms for general aviation aircraft is not an option, as it would significantly increase the cost of such an aircraft. In the small aircraft future avionics architecture (SAFAR) program, an ongoing European project, a low-cost FBW platform will be developed for small aircraft by using technologies originating from the automotive industry. The work in this paper focuses on the design of a FEP control system by trading off several control strategies adopted by industry and academia. As such, it provides a preliminary comparison study among these control strategies and their implications on system requirements, performance, cost, and certification.

This paper is structured as follows. First, a review is provided of FEP strategies and their benefits and pitfalls. Second, the role of the aircraft model fidelity and accuracy on the FEP design will be described. Then, a test case will be presented using classic and advanced control strategies on a low-fidelity aircraft model. Finally, a discussion of the results is provided, followed by the conclusions.

II. Review of Flight Envelope Protection Strategies

Modern FBW control systems have a FEP system that prevents the pilots from entering state and control regions outside the safe flight regime of the aircraft. In this section, a review is provided on several aspects of FEP. First, the determination of the safe flight regime is investigated, both a priori and during flight. Second, four different strategies to protect the aircraft against exceeding its safe flight envelope will be reviewed. These strategies are control limiting, command limiting, using a constrained flight control law (CFCL), and virtual control limiting [7]. Third, the pilot authority at the boundary will be discussed, with the use of soft limits and hard limits.

A. Safe Flight Envelope Definition

The safe flight regime is commonly described in terms of limitations on airspeed, pitch and roll angles, angle of attack, and load factor. Predefining this regime has the advantage that the limits can easily be interpreted and pose little or no sensor requirements. Consider the dynamic aircraft model:

$$\dot{\mathbf{x}} = f(\mathbf{x}, \mathbf{u}) \tag{1}$$

in which $\mathbf{x} \in \mathbb{R}^n$ denotes the state variables of the aircraft and $\mathbf{u} \in \mathbb{R}^m$ the input to the aircraft model. The fixed flight envelope limits (i.e., limitations on the aircraft state) can be written as

$$\underline{\mathbf{x}} \leq \mathbf{x}(t) \leq \bar{\mathbf{x}} \quad \forall\ t \in [0, T] \tag{2}$$

in which $T \geq 0$ is some time horizon. The largest drawback of using a predefined flight envelope is that in case of failures the limits are not accurate anymore. Because of a failure (e.g., actuator hardover, structural damage of the aircraft, etc.), the safe flight envelope will shrink and limits will narrow. When the old boundaries are still used, it cannot be guaranteed that the FEP system will keep the aircraft within the safe flight regime. Tang et al. suggest that it should be possible to use multiple predefined flight envelope sets and let the sensor information determine which set is currently used by the FEP system [8]. The flight envelope limits then become a function of time:

$$\underline{\mathbf{x}}(t) \leq \mathbf{x}(t) \leq \bar{\mathbf{x}}(t) \quad \forall\ t \in [0, T] \tag{3}$$

Tang et al. also use a different approach, in which the safe flight envelope is not defined beforehand but online through reachability and viability calculations [8]. First, an aircraft model is identified online. This model can be used to predict the effects of control surface deflections on state variations [9]. Then, the flight envelope is determined as follows. Let $\mathcal{U}_{[t|t']}$ denote the set of Lebesgue measurable functions from the interval $[t, t']$ to the set of possible inputs $\mathbf{U} \in \mathbb{R}^m$. Given the set of states $\mathbf{K} \in \mathbb{R}^n$, the safe flight envelope can be estimated by gathering the initial states for which the following hold:

1) There exists a $\mathbf{u}(\cdot) \in \mathcal{U}_{[t|T]}$ for which the trajectory $\mathbf{x}(\cdot)$ satisfies $\mathbf{x}(\cdot) \in \mathbf{K}\ \forall\ t \in [0, T]$.

2) There exists a $\mathbf{u}(\cdot) \in \mathcal{U}_{[t|T]}$ and a $t \in [0, T]$ such that the trajectory satisfies $\mathbf{x}(t) \in \mathbf{K}$.

The constraints calculated from the reachable set are then used in the protection system.

B. Flight Envelope Protection

When the flight envelope limits are known, either through online or offline determination, the flight control law (FCL) can be changed and/or extended in order to ensure that the aircraft stays within these boundaries. This section provides details on the four possibilities of FEP shown in Fig. 1: control limiting, command limiting, using a CFCL, and virtual control limiting.

1. *Control Limiting*

In a control limiting setup, an additional block is placed between the FCL and the aircraft, as shown in Fig. 1a. It performs two tasks. First, the envelope limits are mapped onto control surface deflection limits. This mapping is nontrivial and can be done in many ways: by inverting the input–output relation, by using physical functions such as a force equilibrium function, or by approximating the control surface deflection limits by using safe flight envelope margins (i.e., when the aircraft is far away from its limits, large control surface deflections are allowed, and, when close to the limits, control surface deflections are restricted). An advantage of control limiting is that only one set of mapping functions is required for all FCLs, i.e., only from the state limits onto control surface deflection limits, irrespective of which FCL is selected. The second task of the FEP module is to keep the output of the FCL between the calculated control surface deflection limits:

$$\underline{\mathbf{u}}(t) \leq \mathbf{u}(t) \leq \bar{\mathbf{u}}(t) \quad \forall\ t \in [0, T] \tag{4}$$

in which $[\underline{\mathbf{u}}(t)\bar{\mathbf{u}}(t)]^T = \mathbf{m}_{\mathbf{f}:\underline{\mathbf{x}},\bar{\mathbf{x}}\to\underline{\mathbf{u}},\bar{\mathbf{u}}}(\mathbf{x}, \underline{\mathbf{x}}, \bar{\mathbf{x}}, t)$, with $\mathbf{m}_\mathbf{f}$ denoting a set of mapping functions from state constraints onto input constraints. Reaching these control surface deflection limits is similar to reaching actuator limitations and should be included in integrator antiwindup schemes or pseudocontrol hedging [10] schemes of the FCL.

2. *Command Limiting*

In a command limiting setup, an additional block is placed between the stick and the FCL, as shown in Fig. 1b. The FEP block basically performs the same tasks as for control limiting. First, the flight envelope limits are mapped onto command limits. For each control mode, a different set of mapping functions is needed, because different commands will be used for each control mode. This is a drawback of command limiting. The mapping functions themselves tend to be simpler, however. For example, mapping an altitude limit onto an altitude command limit for an altitude hold control law can be done straightforwardly with input saturation. Second, the stick commands are limited before they are fed to the FCL. This has the advantage that no additional integrator windups will occur in the FCLs.

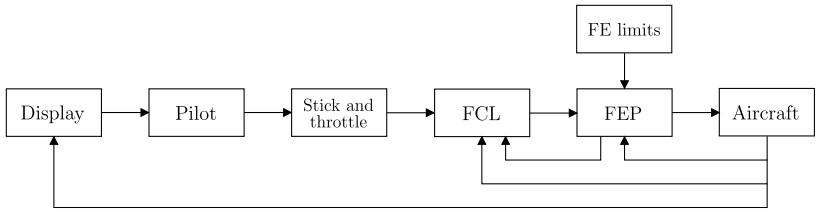

a) FEP using control limiting

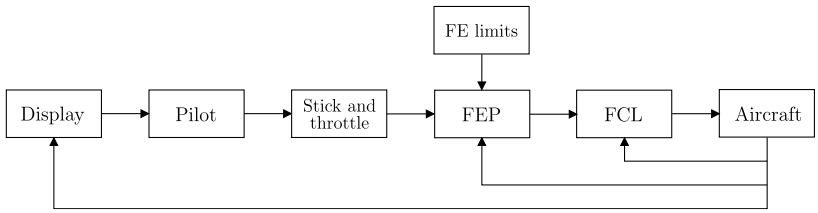

b) FEP using command limiting

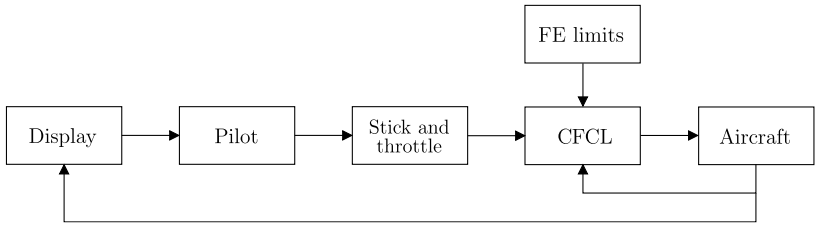

c) FEP using a constrained flight control law

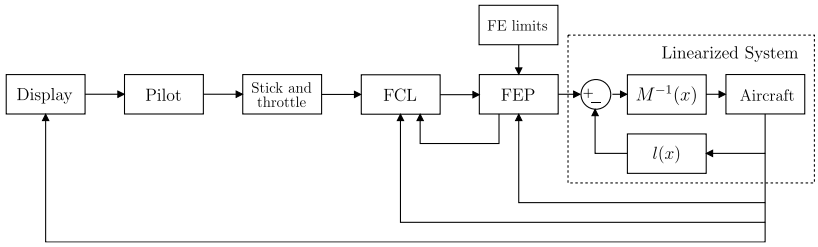

d) FEP using virtual control limiting

Fig. 1 Different strategies for keeping the aircraft within the safe flight envelope.

3. Constrained Flight Control Law

A third way to keep the aircraft within the safe flight envelope is to use a (state) constrained FCL, as shown in Fig. 1c. Model predictive control (MPC) is a perfect candidate for this task, due to its explicit constraint-handling capabilities [11]. Originating from the process industry, MPC is capable of keeping multivariable systems within explicitly defined boundaries while tracking a desired trajectory with high performance [12]. *MPC* is a collective term for several control algorithms in which a dynamic model of the system is used to predict and optimize future states and needed inputs of the system. At each control interval, the MPC algorithm computes an open-loop sequence of the manipulated variables in such a way that the future behavior of the system is optimal. The first value in this optimal sequence is applied as an input to the system, and the optimization process is repeated at the subsequent control intervals [11]. This principle is called the receding horizon principle and is presented graphically in Fig. 2. At time k, an optimal control sequence $\mathbf{u}_{k+i|k}$ is calculated over a prediction horizon H_p, in which the control is assumed to be constant after the input horizon H_u, as shown in Fig. 2a. Only the first element of this sequence is used as an input to the system. Then, the horizon is receded over one sample to $k+1$, and the optimization is repeated with new measurements from the system, giving a new and probably different optimal control sequence as shown in Fig. 2b.

Often, MPC is based on a discrete linear system. For these kinds of systems, future predictions can easily be made by simple matrix multiplications and additions. Consider the discrete linear system:

$$\mathbf{x}_{k+1} = A(k)\mathbf{x}_k + B(k)\mathbf{u}_k \tag{5}$$

Predictions of this system can be written as

$$\begin{bmatrix} \hat{\mathbf{x}}_{k+1|k} \\ \vdots \\ \hat{\mathbf{x}}_{k+Hp|k} \end{bmatrix} = \Psi\mathbf{x}_k + \Upsilon\mathbf{x}_{k-1} + \Theta\Delta\mathbf{U}_k \tag{6}$$

in which

$$\Psi = \begin{bmatrix} A \\ \vdots \\ A^{H_p} \end{bmatrix}, \qquad \Upsilon = \begin{bmatrix} B \\ \vdots \\ \sum_{i=0}^{H_p-1} A^i B \end{bmatrix},$$
$$\Theta = \begin{bmatrix} B & \cdots & 0 \\ \vdots & & \vdots \\ \sum_{i=0}^{H_p-1} A^i B & \cdots & \sum_{i=0}^{H_p-H_u} A^i B \end{bmatrix} \tag{7}$$

The optimal sequence of manipulated variables can be found by solving the quadratic programming (QP) problem:

$$\min_{\Delta\mathbf{U}_k} \Delta\mathbf{U}_k^T(\Theta^T Q\Theta + R)\Delta\mathbf{U}_k - (2\Theta^T Q E_k)^T\Delta\mathbf{U}_k$$
$$\text{subject to } F\Delta\mathbf{U}_k \le \mathbf{c} \tag{8}$$

in which Q and R are weighing matrices, $E(k) = T_k - \Psi x_k - \Upsilon u_{k-1}$ represents the tracking error, and F and $\mathbf{c}$ describe the state, input,

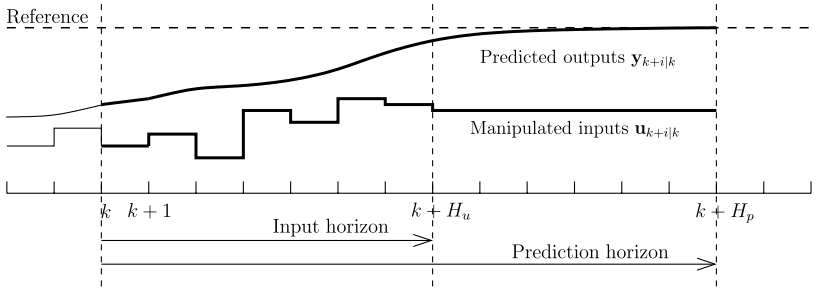

a) Optimal control sequence calculated at time k

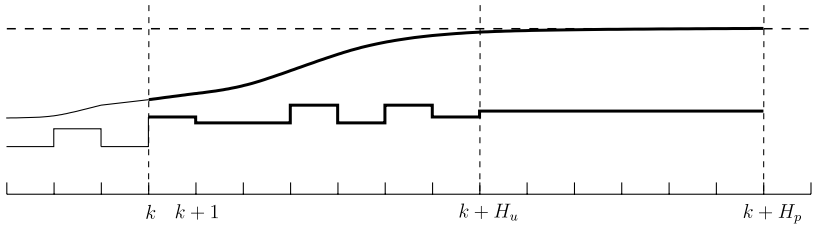

b) New sequence is calculated after receding the horizon

Fig. 2 The receding horizon principle of MPC.

and incremental input constraints on the system. The outcome of the QP solver is either infeasibility or the optimal sequence of manipulated variables of which the first element can be applied to the system. Depending on the number of states of the system and the number of prediction steps used, the matrices may become very large, and solving the QP problem could be time-consuming.

Because of the nonlinearities at the boundaries of the flight envelope, the predictions made using such a linear model are most likely incorrect. Nonlinear MPC exists, but unfortunately it is currently too slow for application in aircraft control [13,14]. An alternative approach often taken is nonlinear dynamic inversion [15,16] (NDI), to obtain almost full linearity of the controllable system, on which a MPC controller can then be applied. NDI is a type of feedback linearization that continuously linearizes the aircraft model by inverting the nonlinear dynamics. The combination of NDI and aircraft dynamics then results in a mere chain of integrators. For demonstration purposes, suppose a nonlinear single input/single output system can be described by

$$\dot{\mathbf{x}} = \mathbf{f}(\mathbf{x}) + \mathbf{g}(\mathbf{x})u \qquad y = h(\mathbf{x}) \tag{9}$$

The control variable y is differentiated with respect to time until it becomes an explicit function of the input. Thus,

$$\dot{y} = \frac{\partial h}{\partial \mathbf{x}}\dot{\mathbf{x}} = \frac{\partial h}{\partial \mathbf{x}}\mathbf{f}(\mathbf{x}) + \frac{\partial h}{\partial \mathbf{x}}\mathbf{g}(\mathbf{x})u \tag{10}$$

Feedback linearization is achieved using the control input:

$$u = M^{-1}(\nu - l) \tag{11}$$

in which $M = (\partial \mathbf{h}/\partial \mathbf{x})\mathbf{g}(\mathbf{x})$ and $l = (\partial \mathbf{h}/\partial \mathbf{x})\mathbf{f}(\mathbf{x})$. Application of this input to the system results in the output y becoming the integral of the virtual control input ν. The linear system $\dot{y} = \nu$ can easily be discretized and then used to predict the future behavior of the system in the MPC controller. Figure 3 shows the principle of NDI in a block diagram.

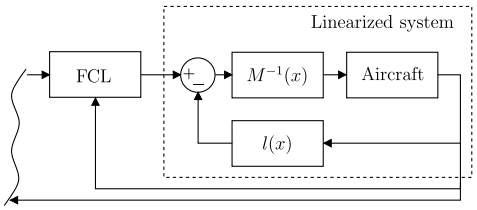

Fig. 3 Feedback linearization using NDI.

For a low-fidelity aircraft model, the nonlinear dynamics are not known very accurately, and, therefore, inversion may be problematic. Using NDI with a linear fractional representation of the uncertainty shows that modeling errors can result in incomplete linearization [17] and, therefore, poor performance of the MPC controller. When NDI on the incremental input of the system is used, a large part of the uncertain parameters drop out. This method, also known as incremental nonlinear dynamic inversion (INDI), thereby decreases the sensitivity to parametric uncertainty [18]. Consider the moment equation:

$$M_a + M_c = J\dot{\omega} + \omega \times J\omega \tag{12}$$

in which M_a represents the aerodynamic moment, M_c the aerodynamic moment due to control surface deflections, J the inertia tensor, and ω the rotational velocity of the aircraft. Suppose that a change in control moment has a far greater effect on the angular acceleration than on the angular rate or, in other words, that time scale separation may be applied [19]. The incremental moment equation can then be written as

$$\partial M_c = J(\dot{\omega}_{\text{new}} - \dot{\omega}_{\text{cur}}) \tag{13}$$

In this equation, the parametric uncertain M_a has dropped out. Using Eq. (13) as a basis for NDI will, therefore, result in a control law that is less sensitive to parametric uncertainty. Equation (13) also shows that application of INDI requires knowledge on the angular accelerations of the aircraft $\dot{\omega}$. There are devices on the market that can measure the angular acceleration, but these are costly. An alternative approach is to use the angular rates available from inertial measurement units and differentiate this signal. This procedure will put requirements on the noise level of that signal, however.

4. Virtual Control Limiting

Application of a feedback linearizing control scheme such as NDI allows for the definition of a fourth FEP strategy, virtual control limiting. In this setup, limitations are not applied on the control surface deflections but on the virtual control input ν of the linearized system, as shown in Fig. 1d. In this way, only one set of mapping functions is needed, i.e., from state constraints onto virtual control input constraints, irrespective of the outer-loop control law used. These functions are likely to be simpler than the mapping functions needed for control limiting and can be written as

$$\underline{\nu}(t) \le \nu(t) \le \bar{\nu}(t) \quad \forall\ t \in [0, T] \tag{14}$$

in which $[\underline{\nu}(t)\bar{\nu}(t)]^T = \mathbf{m}_{\mathbf{f};\underline{\mathbf{x}},\bar{\mathbf{x}}\to\underline{\nu},\bar{\nu}}(\mathbf{x}, \underline{\mathbf{x}}, \bar{\mathbf{x}}, t)$.

C. Pilot Authority at the Boundary

Irrespective of the methods used for determining and protecting the flight envelope, control authority at the boundary must be defined. In commercial aviation control systems, there is a very important distinction between the approaches to FEP being taken by Boeing and Airbus. The Boeing 777 has so-called soft protections, meaning that the crew can override them by using excess force on the control column. Thus, the protection system will make it more difficult to do something it thinks should not be done but will always leave the final decision to the crew. The main advantage of soft limits is that pilots can always operate the aircraft at its full capability whenever required. The disadvantage is that less experienced pilots can always control the aircraft into unsafe flight conditions. In other words, pilots have to be fully aware of the aircraft limitations. Otherwise, they still have the authority to make things worse.

In contrast, the protections on the A320 are so-called hard limits that cannot be overridden. That is, you either get switched into an alternate control mode or your inputs will be ignored. The advantage of hard limits is that the protection system will always keep the aircraft in safe flight regimes and, therefore, controllable, irrespective of pilot control actions. The main disadvantage is that it prevents the aircraft from being operated at its full capacity, which can also have some serious consequences. For example, in the China Airlines B 747 incident 300 n miles northwest of San Francisco, in 1985 [20], the crew was forced to overstress (and structurally damage) the horizontal tail surfaces to recover from a roll and near-vertical dive following an automatic disconnect of the autopilot. At the time of disconnect, full rudder was engaged to one side, and the crew was unaware of this. The crew recovered control with about 10,000 ft of altitude left from an original high-altitude cruise. It is very likely that, if the aircraft had prevented the crew from initiating control commands that would lead to aircraft damage, the aircraft (and passengers) would have been lost.

III. Aircraft Model Requirements

This section provides some remarks on aircraft model requirements related to FEP system design. First, the necessity of a nonlinear model is explained, followed by a brief description on how such a model may be obtained. The last part of this section shows the influence of the mapping functions on the required model accuracy.

A. Importance of Modeling Nonlinearities

In general, much effort is directed into creating an aircraft model suitable for controller design. This is quite logical, because a good aircraft model will require a less robust control law and may, therefore, lead to a better performing controller. It is common practice that controller design is done using linearized aircraft models and classical control theory. Several operating points are selected within the flight envelope, around which the linear approximation is valid. These linearized models are then used in analysis and design tools, such as Root Locus, Bode, Nyquist, etc. For the design of a FEP system, this procedure will probably fail to provide satisfactory results. FEP plays its role at the limits of the flight envelope, where most nonlinear effects are present. Therefore, a full nonlinear model is highly preferred.

B. Obtaining a Nonlinear Model

Linear parameters of a Piper Seneca 2 model, obtained using flight tests during the cruise phase, were available during this study. To create a nonlinear model, different methods may be applied, for example, wind-tunnel tests, computational fluid dynamics computations, or handbook methods based on empirical data. In the 1970s, the United States Air Force combined many handbook methods into a data companion called *DATCOM*. Using this program, the stability and control derivatives can be estimated based solely on the geometric data of the aircraft. Many small aircraft have quite conventional shapes and fly at low (subsonic) velocities. These are precisely the conditions for which DATCOM is known to have good results [21]. After conversion to the body fixed reference frame, DATCOM provides the parameters for the following aerodynamic model:

$$\begin{aligned}
C_X &= C_{X_0} + C_{X_\alpha}\alpha + C_{X_{\delta_e}}\delta_e + C_{X_{\delta_f}}\delta_f \\
C_Y &= C_{Y_\beta}\beta + C_{Y_r}\frac{rb}{2V} \\
C_Z &= C_{Z_0} + C_{Z_\alpha}\alpha + C_{Z_{\dot\alpha}}\dot\alpha + C_{Z_q}\frac{q\bar{c}}{2V} + C_{Z_{\delta_e}}\delta_e + C_{Z_{\delta_f}}\delta_f \\
C_l &= C_{l_\beta}\beta + C_{l_p}\frac{pb}{2V} + C_{l_r}\frac{rb}{2V} + C_{l_{\delta_a}}\delta_a \\
C_m &= C_{m_0} + C_{m_\alpha}\alpha + C_{m_{\dot\alpha}}\dot\alpha + C_{m_q}\frac{q\bar{c}}{2V} + C_{m_{\delta_e}}\delta_e + C_{m_{\delta_f}}\delta_f \\
C_n &= C_{n_\beta}\beta + C_{n_p}\frac{pb}{2V} + C_{n_r}\frac{rb}{2V} + C_{n_{\delta_a}}\delta_a
\end{aligned} \tag{15}$$

Note that the rudder influence on roll $C_{l_{\delta_r}}$ and yaw motion $C_{n_{\delta_r}}$ are not provided by DATCOM and should be added from an alternative source. Figure 4 shows a comparison between the DATCOM results and the linear parameters obtained from flight tests, for a selection of important aerodynamic model parameters. Apparently, most parameters match very well; only C_{m_α} and $C_{m_{\delta_e}}$ differ, by about 50%. To model the nonlinearities at the limits of the flight envelope, the

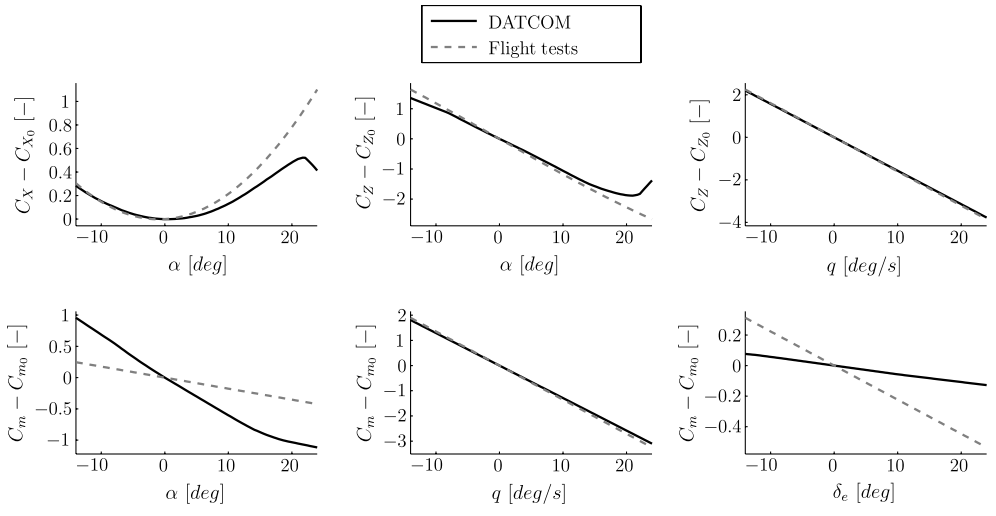

Fig. 4 Comparison of important aerodynamic model parameters for a Piper Seneca 2.

parameters obtained from DATCOM are, therefore, used in the Piper Seneca 2 model.

C. Mapping Functions and Aircraft Model Fidelity

Another requirement on the aircraft model is posed by the choice in mapping functions used in the FEP system. High model accuracy is required when physical functions, or inversed input–output relations, are used as mapping functions. For example, consider the transfer function from elevator deflection angle to pitch angle:

$$H(s) = \frac{\theta(s)}{\delta_e(s)} \tag{16}$$

This relation calculates the elevator deflection corresponding to the upper pitch angle limit:

$$\underline{\delta}_e(s) = H^{-1}(s)\bar{\theta}(s) \tag{17}$$

Clearly, H should be invertible, and it should also be accurate, because there is no correctional term present in the equation. If an inaccurate model is used, the mapping may become inexact, leading to the possibility of exceeding the safe flight envelope.

Using approximation functions, the mapping is more likely to be robust against small model uncertainties, and, therefore, the fidelity of the aircraft model may be lower. For example, suppose an elevator deflection limit can be related to the upper pitch angle limit, as follows:

$$\underline{\delta}_e = \delta_{e,\text{trim}} + K_p(\theta - \bar{\theta}) \tag{18}$$

in which K_p is a proportional gain. This relation is not dependent on model information and is, therefore, less sensitive to model uncertainty. However, the amount of freedom the pilot has within the safe flight envelope may be restricted unnecessarily, because the limits are not determined accurately.

IV. Test Case Definition

The remainder of this paper contains a comparison study. The performance, defined as the ability to keep the aircraft within the safe flight envelope, of four different FEP systems will be compared in the time domain. In this study, knowledge of the aircraft model and of the benefits and pitfalls of FEP strategies will be used to find the FEP system best suited for the test case presented in this section. First, the method of this test case is described. Second, the four FEP options are presented. Third, the results of the test case are given.

A. Method

1. *Aircraft Model*

The aircraft used in the test case is a Piper Seneca 2. The dynamic behavior of a Piper Seneca 2 is captured in a multimodel six-degree-of-freedom nonlinear mathematical model. The aerodynamic model of the aircraft is created using DATCOM+, as mentioned in the previous section. The aerodynamic model is combined with a mass model and a thrust model, supplied by the manufacturer. The aircraft will be trimmed at cruise condition: 120 kt and 6000 ft. Cruise condition is, partly, selected because of the available data but also because most fatal accidents related to handling and control of the aircraft occur during the cruise and maneuvering phase [1]. The majority of all accidents occurs during the landing phase, but, because the energy state of the aircraft (both potential and kinetic) is quite low during landing, many of those accidents are nonfatal.

2. *Flight Control Law*

Direct control of this model (and the aircraft) is not very easy. Part of this is caused by the coupling of aircraft states; for example, banking to the left will also pitch down the nose of the aircraft. An attitude rate command attitude hold (RCAH) control law, as shown in

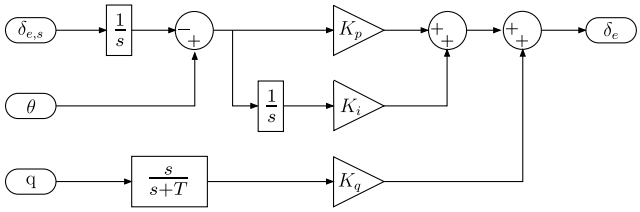

Fig. 5 Attitude RCAH control law.

Fig. 5, will be used as FCL to control the deflection of the elevator and the ailerons. The stick position provides an attitude-rate command to the control law. This command is integrated and then used as a reference. When the attitude is disturbed, e.g., due to turbulence, the reference will not change, and the control law will cancel the disturbance. Turbulence rejection is a very important property of this FCL. A stick displacement in y-direction results in a roll rate command. The pitch rate command will remain zero, however. The change in pitch angle caused by the rolling motion of the aircraft is, therefore, also canceled. In other words, control of the aircraft becomes decoupled. These two properties allow for easy aircraft handling and may be suitable for less experienced pilots. Thorough investigation of the handling qualities is not treated in this text, because the focus here lies on the FEP system. More information on this topic can be found in the work of Mulder et al. [22].

The drawback of a RCAH FCL is that it is not inherently stable. This means that keeping a certain stick deflection will not result in a new equilibrium situation but a constantly changing attitude angle. Even keeping the stick centered is not necessarily safe, because speed stability is removed from the dynamic behavior of the aircraft. Without application of FEP, this behavior is very dangerous. It should, therefore, be a good FCL for this test case.

The rudder deflection and throttle setting are controlled by an autopilot in this test case. The rudder controller will try to minimize the side-slip angle by directly reacting to β, and an autothrottle will try to keep the speed constant by directly reacting to V_{TAS}.

3. *Input Signal*

To test the performance of the FEP systems, a sufficiently large step is given as pitch rate command. This will cause a sharp pull-up maneuver, during which the angle of attack limit is reached, followed by a pitch angle limit. The aircraft will decelerate in this condition until the stall speed limit is reached. After 20 s, the input is reversed to check for integrator windups of the control system.

4. *Flight Envelope Determination*

The selected control law requires the use of FEP for safe flying. However, before the flight envelope can be protected, it must be defined. Restriction to low-cost sensors limits the usefulness of online model identification. The noise of the sensors will lead to uncertainty in the model parameters, resulting in a conservative definition of the flight envelope. Moreover, determination of the flight envelope through reachability and viability calculations is currently too slow for online application. A predefined flight envelope limit set will, therefore, be used in the test case.

5. *Available Mapping Functions*

The four FEP strategies to compare are control limiting, command limiting, replacing the FCL by a CFCL, and virtual control limiting. For all these strategies, a mapping of the state constraints is required. Restriction to low-cost sensors also affects the choice in mapping functions that can be used. The use of physical functions, such as a force equilibrium or an energy conservation function, requires much knowledge of the aircraft state and would, therefore, pose considerable sensor requirements. Mapping functions that use inverted input–output relations are also less useful, because the fidelity of the model used in this test case is not very high. The only mapping functions that can be used are, therefore, approximate mapping functions.

6. Authority at the Boundary

The pilot authority at the envelope boundary is defined using hard limits. In this way, the system is usable for less experienced pilots, because they are not able to structurally damage the aircraft. Furthermore, the use of soft limits would require a force or force-feedback stick, which is more expensive and uses more space in the often already cramped cockpit.

7. Conditions

The goal of this paper is the investigation of practical FEP systems. To increase the practical use of these systems, several off-nominal conditions need to be added to the test case. Because of the low fidelity of the model, robustness to parameter changes is very important. As the input in the test case is a longitudinal one, only longitudinal model parameters need to be altered. To investigate the robustness of the FEP systems to parameter uncertainty, the basic longitudinal force coefficient C_{X_0} is increased by 10%, whereas the influence of the angle of attack on the vertical force coefficient C_{Z_α} is decreased by 10%. From the comparison between DATCOM and flight-test data, it appears that the elevator effectiveness $C_{m_{\delta_e}}$ is somewhat underestimated by DATCOM. Therefore, this parameter is increased by 40%. Mass m and longitudinal center-of-gravity position x_{cg} are also subject to change during flight and have, therefore, been increased by 10 and 5%, respectively.

The use of low-cost sensors brings about the necessity to deal with noisy signals. Investigating the sensitivity to sensor noise is, therefore, crucial. The output of the aircraft is modified using first- or second-order sensor dynamics, an appropriate level of filtered zero mean white noise, and a constant bias. The output of this sensor block is fed to the control system.

Besides sensor noise, time delays of the signals can have a severe impact on the performance of the FEP systems. Sensitivity to these delays is investigated using transport delays of 50, 100, and 150 ms.

The final off-nominal condition examined in this paper is flying through turbulence and wind gusts. This condition causes disturbances on the input, as seen from the controller. It is, therefore, similar to the condition with sensor dynamics; however, the frequency and amplitude of the disturbance are completely different. Because the effect of turbulence on small aircraft is profound, this condition could have a large impact on the FEP system. The effects of turbulence have been modeled according to the mathematical representation in Sec. 3.7 of the military specification MIL-F-8785C [23]. The intensity of the applied turbulence is labeled as "moderate" by MIL-F-8785C. This means that, at an altitude of 6000 ft, the root mean square of the turbulence intensity is 3 m/s. Accounting for the turbulence scale length of 533.4 m and the aircraft velocity of 62 m/s, the amplitude of the vertical turbulence component is around $w_{\text{turb}} = \pm 3\sqrt{533.4/(62\pi)} = \pm 5$ m/s. A rough approximation of the maximum change in angle of attack caused by this turbulence, neglecting the horizontal turbulence component and assuming $u \approx V$, is, therefore, $\alpha_{\text{turb}} = \arctan(5/62) = 0.08$ rad or 4.6 deg. The wind gust used in this condition is defined by MIL-F-8785C as a "1-cosine" shape. It starts after 10 s, at which time $V = 50$ m/s and has a buildup length of 120 m and an amplitude of 3.5 m/s, in X_B-direction, and 3.0 m/s, in Z_B-direction. The change in angle of attack due to this gust is approximately $\alpha_{\text{gust}} = \arctan(3/(50 - 3.5)) = 0.063$ rad or 3.6 deg.

B. Flight Envelope Protection Strategies

1. Control Limiting

In the control limiting setup, multiple parallel proportional-integral-derivative (PID) controllers, one for each flight envelope limit, can be used for the mapping of state constraints onto control surface deflection constraint, as shown in Fig. 6. The output of each PID controller is interpreted as a control surface limit. For example,

$$\underline{\delta}_e = \delta_{e,\text{trim}} + K_p(\theta - \bar{\theta}) + K_i \int (\theta - \bar{\theta})\,\mathrm{d}t + K_d \frac{\mathrm{d}(\theta - \bar{\theta})}{\mathrm{d}t} \tag{19}$$

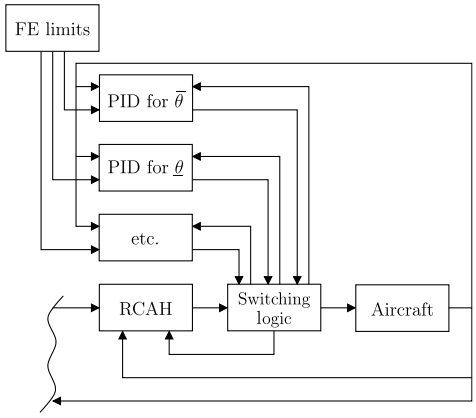

Fig. 6 Control limiting using multiple PID controllers.

in which K_p, K_i, and K_d are gains. Note that in order to prevent "suction" toward the limit while being in the safe flight envelope, the integral should be kept zero until the limit is reached. When the output of the currently selected FCL exceeds a control surface limit, control is switched to that limit hold controller. Additional switching logic is used to return control authority to the pilot on input reversal and prevent integrator windups in the FCL and in the parallel PID controllers.

2. Command Limiting

The second candidate is the command limiting setup, shown in Fig. 7. In this setup, the FEP controller will limit the attitude-rate commands fed to the FCL. The pitch angle limits are mapped onto pitch rate command limits, using parameter projection [24]. Let $\mathcal{S}$ be a convex region defined as

$$\mathcal{S} \triangleq \{\gamma \in \mathbb{R}^{p_\gamma} | \mathbf{g}(\gamma) \leq \mathbf{0}\} \tag{20}$$

in which $g: \mathbb{R}^{p_\gamma} \to \mathbb{R}$ is a smooth function. Parameter projection provides that the parameter γ will remain in $\mathcal{S}$ when

$$\dot{\gamma} = \begin{cases} \dot{\gamma} & \text{if } \gamma \in \mathcal{S}^0 \\ & \text{or if } \gamma \in \delta\mathcal{S} \text{ and } \nabla g^T \dot{\gamma} \leq \mathbf{0} \\ \dot{\gamma} - \Gamma \frac{\nabla \mathbf{g} \nabla \mathbf{g}^T}{\nabla \mathbf{g}^T \Gamma \nabla \mathbf{g}} \dot{\gamma} & \text{otherwise} \end{cases} \tag{21}$$

in which $\mathcal{S}^0$ is the interior of $\mathcal{S}$, $\delta\mathcal{S}$ is the boundary of $\mathcal{S}$, $\nabla \mathbf{g} = \mathrm{d}\mathbf{g}/\mathrm{d}\gamma$, and Γ is a design parameter. In the case of mapping the pitch angle limit onto a pitch rate constraint, the following relations can be used. Because g is a scalar function per parameter, first the upper and lower limits need to be captured in a single function:

$$\begin{aligned} g &= (\theta - (\bar{\theta} + \underline{\theta})/2)^2 - (\bar{\theta} - (\bar{\theta} + \underline{\theta})/2)^2 \\ \nabla g &= 2(\theta - (\bar{\theta} + \underline{\theta})/2) \end{aligned} \tag{22}$$

The pitch angle limits can then be mapped onto pitch rate constraints using

$$q_{\text{cmd}} = \begin{cases} q_{\text{cmd}} & \text{if } g \leq 0 \\ & \text{or if } g = 0 \text{ and } \nabla g q_{\text{cmd}} \leq 0 \\ 0 & \text{otherwise} \end{cases} \tag{23}$$

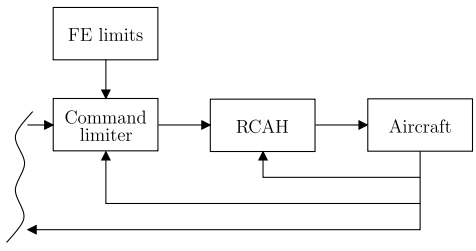

Fig. 7 Command Limiting.

To prevent the aircraft from stalling, the upper pitch angle limit can be decreased on approaching the stall speed $\underline{V}$. This may be done using a hyperbolic tangent function:

$$\bar{\theta} = \bar{\theta} \cdot \tanh\left(c_1 + \frac{V - \underline{V}}{c_2}\right) \tag{24}$$

in which c_1 is a tuning parameter that influences the highest pitch angle allowed at the stall speed limit, and c_2 is a tuning parameter that influences the aggressiveness of the FEP controller on reaching the stall speed limit. Similar constructions are possible for the overspeed, angle of attack, and load factor limits.

3. Constrained Flight Control Law

In the third candidate, the PID FCL is replaced by a MPC controller combined with INDI. This candidate is referred to as CFCL, hereafter. The INDI control variables have to be chosen carefully, because they affect the required mapping of the flight envelope limits onto the controller constraints. Here, the state and input vectors of the linear system used by the MPC controller are chosen as follows:

$$\zeta = \begin{bmatrix} \phi \\ \theta \end{bmatrix}, \qquad \nu = \begin{bmatrix} \dot{p} \\ \dot{q} \end{bmatrix}$$

In this way, the pitch and bank angle limits can be fed straight to the MPC as state constraints. The other aircraft state limits can be protected using the same construction as used in the command limiting setup, i.e., hyperbolic tangent functions. Figure 8 shows the CFCL in a block diagram.

4. Virtual Control Limiting

In the fourth and last candidate, the RCAH FCL is combined with INDI. Again, INDI linearizes the system using differentiated angular rate feedback. The linearized system has the virtual-input variables $\nu = [\,\dot{p} \quad \dot{q}\,]^T$. Adaptation of the gains of the FCL is needed, because the output of the FCL changes from δ_e to $\dot{q}$, but the structure remains the same. FEP is achieved by mapping the state constraints onto angular acceleration constraints, using parameter projection and hyperbolic tangent functions. The control-authority switching logic is copied from the control limiting FEP strategy. Figure 9 shows the FEP strategy in a block diagram.

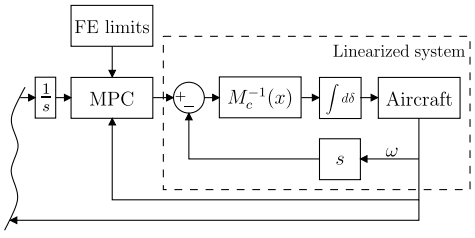

Fig. 8 Replacing the FCL by MPC plus INDI.

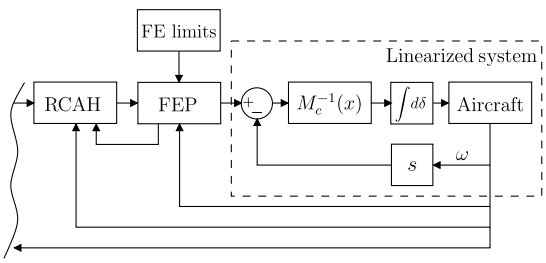

Fig. 9 Virtual control limiting.

C. Results

The performance of the multiple PID control limiting, the command limiting, the CFCL, and the virtual control limiting FEP systems is shown in Fig. 10. This figure also shows the input signal in a solid light grey line and the safe flight envelope limits in a solid black line. Figure 11 shows the performance of the same systems, but now using altered aircraft model parameters. Figure 12 shows the effect of sensor noise, and Fig. 13 shows that of time delays. Figures 14 and 15 show the aircraft response in the presence of wind gusts and turbulence. The results are discussed in detail in the following section.

V. Discussion

A. Performance

The aircraft response to the earlier defined input, using the different FEP systems, is shown in Fig. 10. It should be noted that the PID control limiting setup slightly overshoots the envelope limits. This is quite logical, because each controller activates after the limit has been reached and acts only as a hold controller. When using control limiting, the safe flight envelope must, therefore, be chosen conservatively. In the command limiting setup, the controllers are already active when approaching the limit, and they prevent overshoot. This results in a very smooth interception of the limits, which is preferable for ride comfort and pilot awareness of approaching flight envelope limits. There is barely any difference between the command limiting setup and CFCL setup. Using the virtual control limiting strategy, the pitch angle also overshoots its limit. However, the overshoot is smaller, compared with normal control limiting, because the limit mapping functions are more exact. The response clearly shows that the velocity limit is handled using the same hyperbolic tangent functions used in the command limiting and CFCL setup. All four controllers do not suffer from integrator windups, and control is returned to the pilot immediately after input reversal.

B. Sensitivity to Parametric Uncertainty

Not only is good performance required, but also robustness against modeling errors is crucial for practical use of the FEP system. Figure 11 shows the performance of the controllers in the presence of modeling errors. The control limiting setup is reasonably robust but does get influenced by the uncertainties. Limits are exceeded slightly further, and limit transitions, such as from pitch limit to stall speed limit, oscillate more. This fact can be explained, by realizing that the mapping from state limits onto control surface deflection limits is largely dependent on the control surface effectiveness. Modifying the control surface effectiveness alters the state change caused by a control surface deflection and would, therefore, require a change in mapping. The command limiting, CFCL, and virtual control limiting setups are not sensitive to the changes in the altered parameters. For these setups, the control laws handle the parameter changes, and the mapping functions are not influenced. Because the aircraft was not retrimmed after the model changes, some initial movement can be seen in the first 2 s for all FEP strategies.

C. Sensitivity to Sensor Noise and Bias

A low-cost system implies using low-cost hardware. Unfortunately, low-cost hardware is likely to have much sensor noise and bias. Figure 12 shows the performance of the controllers in the presence of these disturbances. Clearly, the performance of the control limiting FEP system is unsatisfactory. The reason for this lies in the mapping of the velocity constraint onto the elevator deflection limit. The differential term of this hold controller is quite large, and in the presence of sensor noise this signal blows up. Figure 12b shows the aircraft response when stall speed protection is disabled for the control limiting FEP system. The result is considerably better. For the command limiting setup, the added sensor noise and bias hardly influence the response of the aircraft. Although sensitivity to noise on the angular rate measurements was expected for the setups using INDI, the figure does not reflect this. Because the actuator dynamics

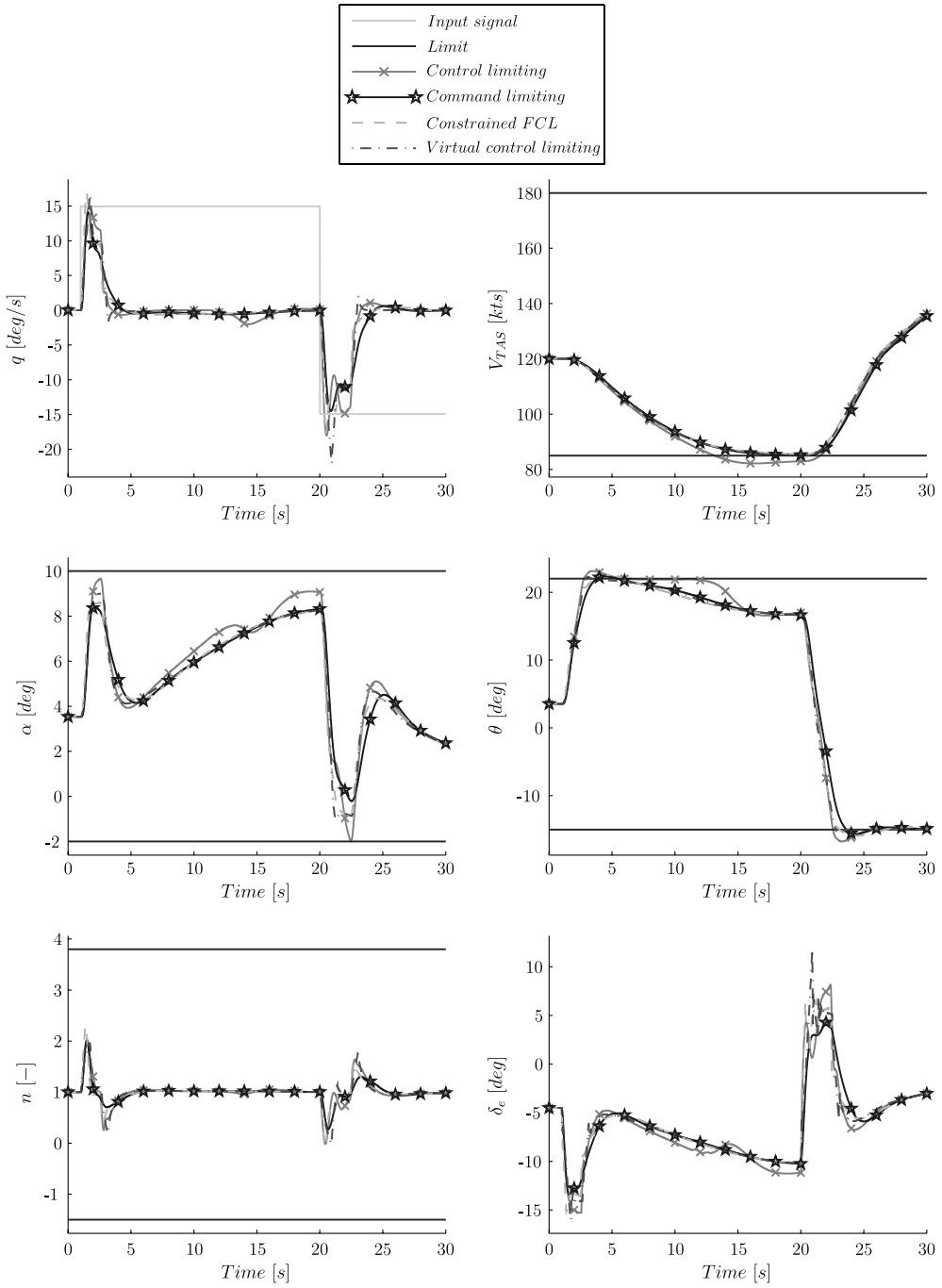

Fig. 10 Aircraft response using different FEP strategies.

act as a low-pass filter, the level of noise applied in this test case does not lead to significant problems.

D. Sensitivity to Time Delays

Besides sensor noise and bias, time delays play a significant role in a low-cost general aviation FBW system. The influence of time delays on aircraft responses is shown in Fig. 13. Figure 13a shows that all systems are hardly influenced by time delays smaller than 50 ms. In the presence of 100 and 150 ms time delays, problems arise, as can be seen in Figs. 13b and 13c, respectively. Both the control limiting system and the CFCL system show rapid oscillations in the pitch angle. The virtual control limiting setup causes an even more sluggish response to the input. All systems do succeed at keeping the aircraft within the safe flight envelope, but ride comfort may be affected. Command limiting is the only FEP system that is influenced only a little in the presence of time delays.

E. Sensitivity to Wind Gusts and Turbulence

Figure 14 shows the influence of wind gusts on the aircraft responses. The angle of attack buildup after 10 s, due to the wind gust, is clearly shown in the response. The FEP controllers prevent the aircraft from exceeding the angle of attack limit, by lowering the nose of the aircraft. The CFCL performs best for this test case, by lowering the nose such that the angle of attack limit is not reached. The command limiting and virtual control limiting controllers push the nose less far down, and this results in a slight overshoot of the angle of attack limit. This behavior comes from a tuning choice, in which a tradeoff is made between the allowance of rapid aircraft responses and strict enforcement of the limitations. The control limiting FEP system reacts after the limit has been exceeded, but it does push the nose down as far as the CFCL controller.

Figure 15 shows the influence of turbulence on the aircraft responses. The influence of turbulence on the angle of attack is attenuated by deflections of the elevator. The RCAH FCL clearly

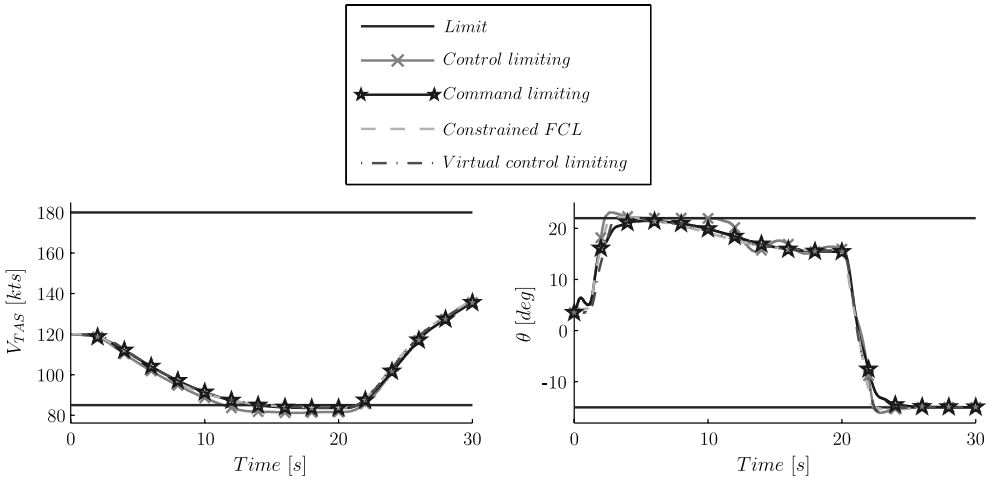

Fig. 11 Aircraft response using different FEP strategies, sensitivity to parametric uncertainty.

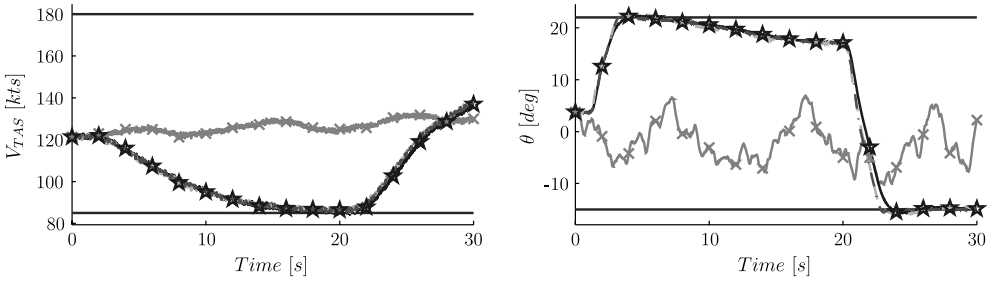

a) Control limiting with stall speed protection

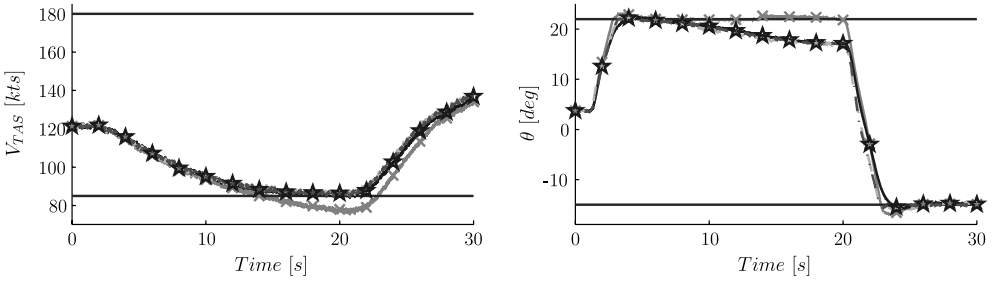

b) Control limiting without stall speed protection

Fig. 12 Aircraft response using different FEP strategies, sensitivity to sensor noise.

rejects the turbulence, as the response of the aircraft is highly similar to the nominal case. All FEP controllers are able to keep the aircraft within the flight envelope limits.

F. Implications for Small Aircraft

The cost of a FEP system is largely determined by sensor requirements and certification costs. Using predefined flight envelope limits and approximate mapping functions results in low sensor requirements and, therefore, potential cost savings. In terms of certification, predefined limits increase the functional visibility of the control system and are, therefore, also advisable. The choice between application of control limiting, command limiting, CFCL, and virtual control limiting is influenced by certification considerations, as well. CFCL has lower functional visibility, mainly due to the use of a QP solver in the MPC controller, and, therefore, requires a more extensive certification procedure than the other controllers [25]. In both INDI setups, matrix inversion is required, which is potentially unstable. However, in the presented test case the matrix inverse always exists, because a linear relation is assumed between the aerodynamic moments and the control surface deflections, and cruise condition is selected as the operating point. A smaller part of the total cost is determined by flight control system hardware. Using CFCL poses a much higher demand on processing power than using PID controllers, which means that more expensive hardware is needed.

G. Scope of the Test Case

The ultimate goal of a practical FEP system is, of course, to be used in real flight. In the SAFAR project, the objective is to install low-cost FBW technology in a Diamond DA42 demonstrator aircraft. As a first step, the FBW system will be switched on during cruise flight, and a conservative set of limits will be used. On this platform, a RCAH FCL combined with a FEP system will aim to make flying this small aircraft easier and safer. This paper contributes to the selection of that FEP system.

The test case presented in this paper, therefore, suits the needs of the project. If the FBW system is used for full flight, additional requirements are posed on the FCL, and RCAH may not be a good choice anymore. This will have an impact on the mapping functions used in the FEP systems and may lead to different results. Also, the

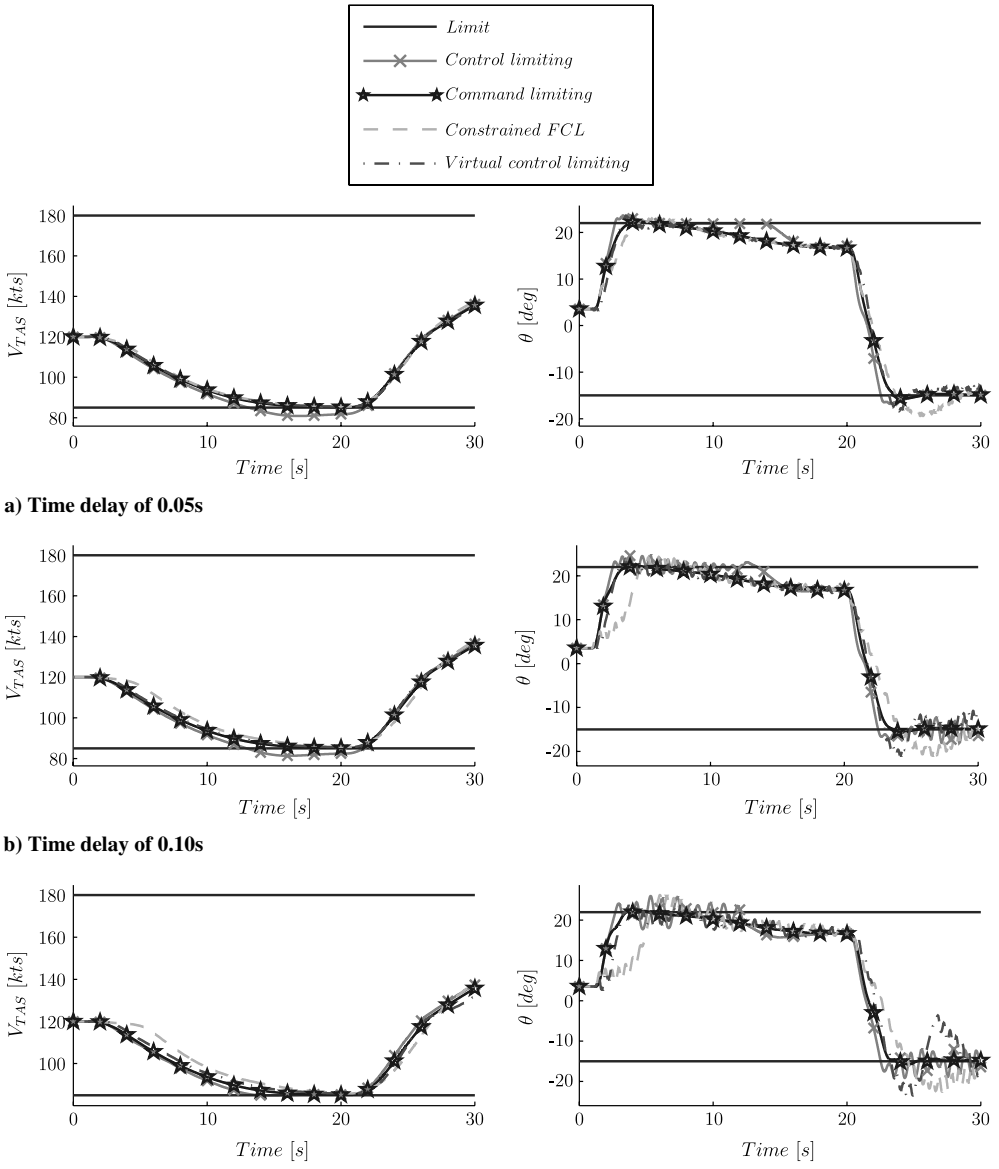

a) Time delay of 0.05s

b) Time delay of 0.10s

c) Time delay of 0.15s

Fig. 13 Aircraft response using different FEP strategies, sensitivity to time delay.

degree of nonlinearity of the model will increase, making the INDI-based systems potentially much more beneficial.

H. Future Investigations

If installment of FBW and FEP contributes to decreasing the rate of handling and control accidents in cruise flight, focus can be diverted to the next major source of accidents. In general aviation, as well as commercial aviation, planning and decision errors are responsible for a large part of the accidents. Much attention is already paid to solving these issues for civil aircraft, and future investigations are needed into the applicability of these solutions to the small aircraft market.

On the other hand, many nonfatal accidents occur during the landing phase. Before personal air transportation is a viable option, this figure must also be reduced drastically. In commercial aviation, autoland systems are installed to prevent landing phase accidents. This solution requires the support of costly airport services, however. A typical airport at which a general aviation aircraft will land probably lacks this support. Therefore, future investigations are needed into landing aid systems to support landing on airports without an instrument landing system. Perhaps, renewed research into global-navigation-satellite-system-based landing systems [26] and/or research into display enhancements [27] can lead to landing aid systems for these situations.

VI. Conclusions

This paper presents a study of FEP techniques for small aircraft. A comparison is made between a PID-based control limiting approach, a command limiting approach, a CFCL approach using MPC combined with INDI, and a virtual control limiting approach using INDI. All four controllers perform well, when there are no model uncertainties present. However, full certainty is hardly the case when a low-cost system is considered. Model parameters are altered up to 40%, and the test case is rerun without adapting the controllers. Command limiting, CFCL, and virtual control limiting proved far less sensitive to parametric changes than the control limiting setup. Similar results are obtained, when sensor noise and bias are considered. Especially, the stall speed protection of the control limiting system proved highly sensitive to sensor noise and bias. In the presence of time delays, only command limiting keeps performing well. The FEP controllers are all able to deal with atmospheric conditions, such as wind gusts and turbulence. Robustness against off-nominal conditions is not the only prerequisite for a well-functioning low-cost

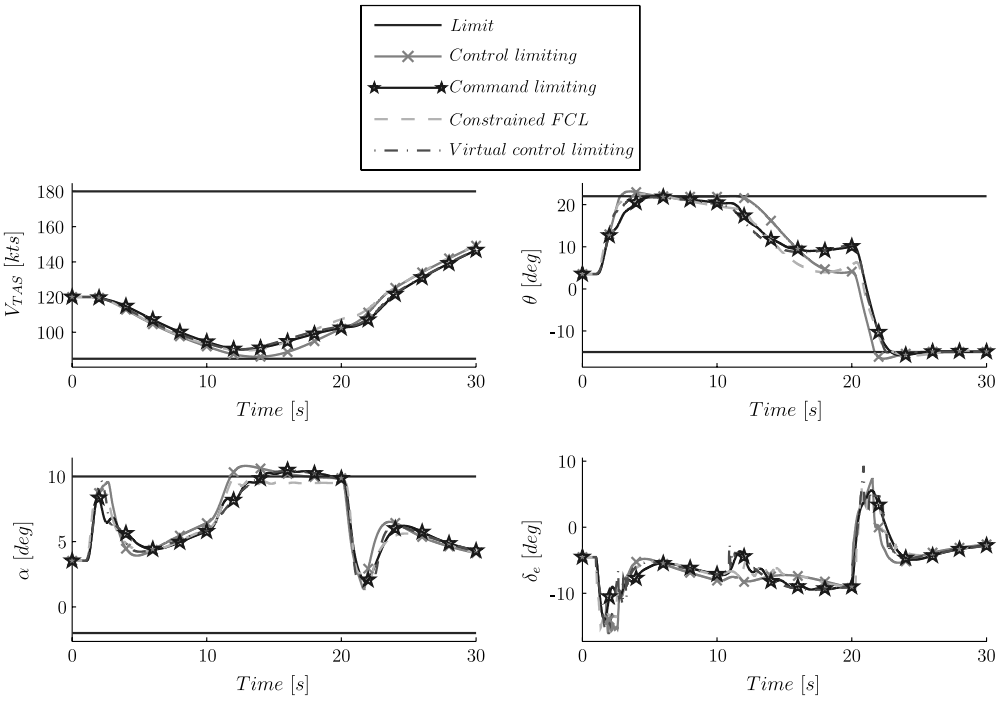

Fig. 14 Aircraft response using different FEP strategies, sensitivity to wind gusts.

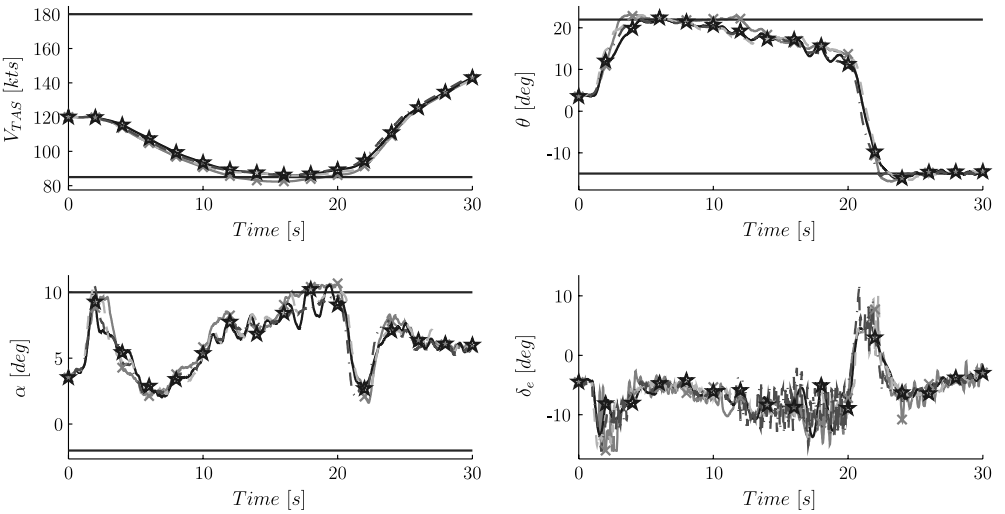

Fig. 15 Aircraft response using different FEP strategies, sensitivity to turbulence.

FEP system, however. CFCL and virtual control limiting have lower functional visibility. Therefore, they are harder to certify and will be more expensive than the command and control limiting setups. Also, the hardware requirements of the CFCL are higher, due to the QP solver used in MPC, making this setup slightly more expensive. Weighing all these considerations leads to the conclusion that command limiting is the preferred option for the chosen test case.

References

[1] "Annual Review of Aircraft Accident Data, U.S. General Aviation, Calendar Year 2005," National Transportation Safety Board Rept. NTSB/ARG-09/01, Washington, D.C., 26 May 2009.

[2] Wiegmann, D. A., Shappell, S. A., Boquet, A., Detwiler, C., Holcomb, K., and Faaborg, T., "Human Error and General Aviation Accidents: A Comprehensive, Fine-Grained Analysis Using HFACS," Aviation Human Factors Div. Inst. of Aviation TR AHFD-05-08/FAA-05-03, Savoy, IL, May 2005.

[3] Dekker, S. W. A., *The Field Guide to Human Error Investigations*, Ashgate, Surrey, England, U.K., 2002, chap. 14, pp. 135–158.

[4] Borst, C., Mulder, M., Van Paassen, M. M., and Mulder, J. A., "An Ecological Approach to Support Pilot Terrain Awareness After Total Engine Failure," *Journal of Aircraft*, Vol. 45, No. 1, 2008, pp. 159–171. doi:10.2514/1.30214

[5] Van Dam, S. B. J., Mulder, M., and Van Paassen, M. M., "Ecological Interface Design of a Tactical Airborne Separation Assistance Tool," *IEEE Transactions on Systems, Man, and Cybernetics, Part A*, Vol. 38, No. 6, 2008, pp. 1221–1233. doi:10.1109/TSMCA.2008.2001069

[6] Traverse, P., Lacaze, I., and Souyris, J., "Airbus Fly-by-Wire: A Total Approach to Dependability," *International Federation for Information Processing*, Vol. 156, 2004, pp. 191–212.

[7] Unnikrishnan, S., *Adaptive Envelope Protection Methods for Aircraft*, Ph.D. Dissertation, Georgia Inst. of Technology, School of Aerospace Engineering, Aug. 2006.

[8] Tang, L., Roemer, M., Ge, J., Crassidis, A., Prasad, J., and Belcastro, C., "Methodologies for Adaptive Flight Envelope Estimation and Protection," AIAA Guidance, Navigation, and Control Conference and Exhibit, AIAA Paper 2009-6260, 2009.

[9] Lombaerts, T., Huisman, H., Chu, Q., Mulder, J., and Joosten, D., "Nonlinear Reconfiguring Flight Control Based on On-Line Physical Model Identification," *Journal of Guidance, Control, and Dynamics*, Vol. 32, No. 3, May–June 2009, pp. 727–748.

doi:10.2514/1.40788
[10] Johnson, E., "Limited Authority Adaptive Flight Control," Ph.D. Dissertation, Georgia Inst. of Technology, School of Aerospace Engineering, Nov. 2000, chap. 2, pp. 15–39.
[11] Maciejowski, J. M., *Predictive Control with Constraints*, Prentice–Hall, Upper Saddle River, NJ, 2002, chaps. 1–3, pp. 1–107.
[12] Qin, S. J., and Badgwell, T. A., "A Survey of Industrial Model Predictive Control Technology," *Control Engineering Practice*, Vol. 11, No. 7, 2003, pp. 733–764.
doi:10.1016/S0967-0661(02)00186-7
[13] Henson, M., "Nonlinear Model Predictive Control: Current Status and Future Directions," *Computers and Chemical Engineering*, Vol. 23, No. 2, 1998, pp. 187–202.
doi:10.1016/S0098-1354(98)00260-9
[14] Allgöwer, F., and Zheng, A., *Nonlinear Model Predictive Control*, Birkhäuser–Verlag, Basel, Switzerland, 2000, pp. 219–245.
[15] Slotine, J.-J. E., and Li, W., *Applied Nonlinear Control*, Prentice–Hall, Upper Saddle River, NJ, 1991, chap. 6, pp. 207–275.
[16] Isidori, A., *Nonlinear Control Systems*, Springer–Verlag, New York, 1995, chap. 4, pp. 137–218.
[17] Van Oort, E., Chu, Q. P., and Mulder, J. A., "Robust Model Predictive Control of a Feedback Linearized F-16/MATV Aircraft Model," AIAA Guidance, Navigation, and Control Conference and Exhibit, AIAA Paper 2006-6318, 2006.
[18] Bacon, B. J., Ostroff, A. J., and Joshi, S. M., "Reconfigurable NDI Controller Using Inertial Sensor Failure Detection and Isolation," *IEEE Transactions on Aerospace and Electronic Systems*, Vol. 37, No. 4, Oct. 2001, pp. 1373–1383.
doi:10.1109/7.976972
[19] Reiner, J., Balas, G. J., and Garrard, W. L., "Flight Control Design Using Robust Dynamic Inversion and Time-Scale Separation," *Automatica*, Vol. 32, No. 11, 1996, pp. 1493–1504.
doi:10.1016/S0005-1098(96)00101-X
[20] "Aircraft Accident Report: China Airlines Boeing 747-SP," National Transportation Safety Board Rept. AAR-86/03, Washington, D.C., 1985.
[21] Hoak, D. E., and Ellison, E. E., "USAF Stability and Control Datcom (and Subsequent Revisions)," U.S. Air Force TR WADD-TR-60-261, 1965.
[22] Mulder, M., Veldhuijzen, A. R., Van Paassen, M. M., and Mulder, J. A., "Integrating Fly-by-Wire Controls with Perspective Flight-Path Displays," *Journal of Guidance, Control, and Dynamics*, Vol. 28, No. 6, Nov.–Dec. 2005, pp. 1263–1274.
doi:10.2514/1.12617
[23] MilSpec, Military Specification: Flying Qualities of Piloted Airplanes, U.S. Military, 05 Nov. 1980, Sec. 3.7.
[24] Krstić, M., Kanellakopoulos, I., and Kokotović, P. V., *Nonlinear and Adaptive Control Design*, Wiley, New York, 1995, pp. 511–514.
[25] Pratt, R., *Flight Control Systems: Practical Issues in Design and Implementation*, Inst. of Electrical Engineers, Herts, England, U.K., 2000, p. 173.
[26] Parkinson, B. W., and Fitzgibbon, K. T., "Aircraft Automatic Landing Systems Using GPS," *Journal of Navigation*, Vol. 42, No. 1, 1989, pp. 47–59.
doi:10.1017/S0373463300015083
[27] Le Ngoc, L., Borst, C., Mulder, M., and Van Paassen, M. M., "The Effect of Synthetic Vision Enhancements on Landing Flare Performance," AIAA Guidance, Navigation, and Control Conference, AIAA Paper 2010-8170, Toronto, 2–5 Aug. 2010.